ELECTRICITY SPOT PRICE MODELLING WITH A VIEW TOWARDS EXTREME SPIKE RISK

CLAUDIA KLÜPPELBERG, THILO MEYER-BRANDIS, AND ANDREA SCHMIDT

Abstract. Sums of Lévy-driven Ornstein-Uhlenbeck processes seem appropriate for modelling electricity spot price data. In this paper we present a new estimation method with particular emphasis on capturing the high peaks, which is one of the stylized features of such data. After introducing our method we show it at work for the EEX Phelix Base electricity price index. We also present a small simulation study to show the performance of our estimation procedure.

1. Introduction

In the last decade, a number of countries have liberalized their electric power sectors. Before, most power sectors were not free to competition, and prices were set by regulators according to the cost of generation, transmission and distribution. Therefore, no price risks existed. Since the liberalization, most electricity is bought through bilateral agreements, i.e. two market participants negotiate prices for the delivery of electricity over one or two years. Another share is bought and sold on spot markets of energy exchanges, where electricity for delivery on the next day is traded. For example, in the European Union the liberalization of power markets has been driven by the directive 96/92/EC of the European Parliament and the European Council. The directive is aimed at opening up the member states' electricity markets, so that an increasing number of suppliers and consumers can have the opportunity to freely negotiate the purchase and sale of electricity. Since 1990, a large number of electricity exchanges have opened in Europe, where prices are determined purely by supply and demand, the major ones listed in Table 1. In addition to next-day-delivery of electricity, some of these exchanges (e.g. Nordpool and EEX) also operate a financial market, where electricity derivatives are traded.

Electricity exchanges trade power generated by different sources, e.g. nuclear power, power from coal, fuel or gas plants, or hydro and wind power. The composition varies between different countries. Figures 1 and 2 show energy sources for Germany and Scandinavia as examples. Almost half of the electricity generated in Scandinavian countries is hydropower, whereas the biggest share of the German power supply is generated by burning coal.

Date: December 28, 2008.

Key words and phrases. Electricity markets, electricity spot price model, estimation of Ornstein-Uhlenbeck processes, extreme value theory, mixture model, Ornstein-Uhlenbeck process, POT method.

Country	Date	Name
England and Wales	1990	Electricity pool
	2001	UK Power Exchange (UKPX)
Norway	1993	Nord Pool
Spain	1998	OMEL
Netherlands	1999	Amsterdam Power Exchange (APX)
Germany	2000	Leipzig Power Exchange (LPX)
	2001	European Power Exchange (EEX)
Poland	2000	Polish Power Exchange
France	2001	Powernext
Italy	2004	Gestore Mercato Elettrico (GME)

TABLE 1. European electricity exchanges and their respective starting years (taken from [7], p. 259)

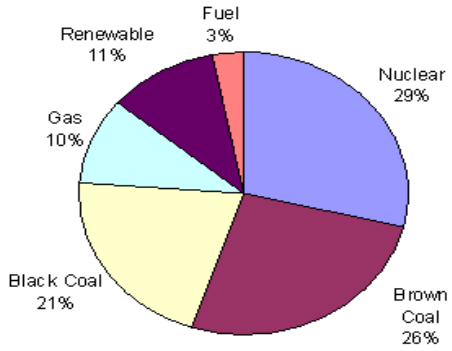

FIGURE 1. Composition of electricity sources in Germany, 2005. Source: VDEW (2006)

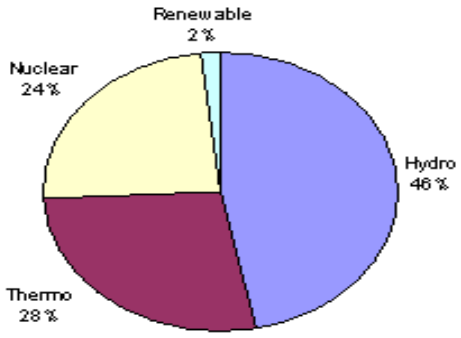

FIGURE 2. Composition of electricity sources in Scandinavia, 2005. Source: Nordel (2007)

The electricity composition is relevant for electricity prices as generating costs vary between energy sources, different cost structures also determine the role of a particular energy source. Nuclear power and hydro energy have high fix costs and relatively low variable costs, so that each extra unit of electricity can be generated at a low price. Thus, both are used to cover the base electricity demand. Coal and gas power plants on the other hand have relatively low fixed costs but high variable costs, so that each extra unit is more expensive than nuclear power and depends on prices for commodities and CO_2 allowances. Consequently, thermo energy is usually used to cover peak demand during the day. Very high demand levels are usually met by burning fuel. Figure 3 visualizes the cost structure, as it is described in [15].

In contrast to most other commodities, the main characteristic of electricity is its very limited storability. It is hardly possible to insure against price risks by building reserves.

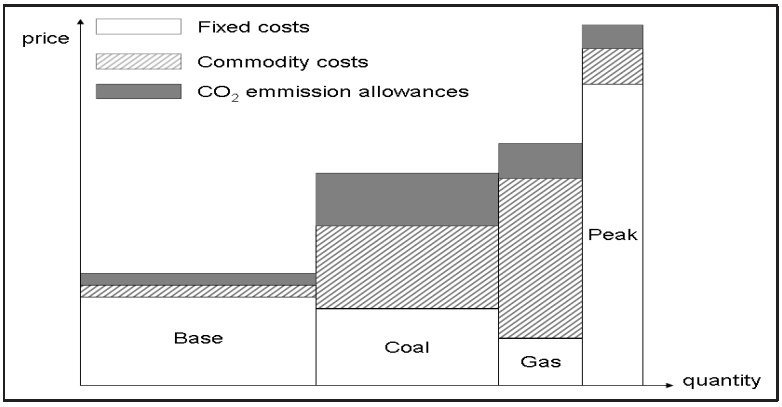

FIGURE 3. Cost Structure. Source: von Hirschhausen et al. (2007)

As a consequence, a sudden rise in electricity demand (e.g. due to weather conditions) or a production drop (e.g. due to a failure of a power plant) have to be compensated by generation sources with often extremely high marginal costs. In times of parallel demand and/or supply shifts, this exploding marginal cost structure together with very inelastic demand then results in impressive price jumps, most often followed by a rather quick return of prices to normal levels. These so called price spikes, which are unique to electricity spot prices, are observed frequently in most electricity markets (see e.g. Figure 5 for EEX spot prices). Obviously, these price spikes constitute a significant risk to energy market participants, and a successful risk management requires among others to appropriately account for spike risk.

In [3], an arithmetic multi-factor non-Gaussian Ornstein-Uhlenbeck model of electricity spot prices is proposed. This model is designed to reproduce path and distributional properties of spot prices, among them spike behavior (see Section 2 for a description of stylized features of spot prices). At the same time, due to the arithmetic structure, the model is analytically tractable. For example, if one makes the usual assumption of a structure preserving risk neutral pricing measure (in the sense that the model is also of arithmetic nature under the risk neutral pricing measure), one obtains closed form formulas for electricity futures and other derivatives prices. See [3] for more details on this. However, since the model is non-Markovian, the question how to estimate the model statistically is not obvious and was left open in [3]. The purpose of this paper is now to propose an estimation procedure for this model, where we focus in particular on appropriate modelling of spike risk. To this end we employ tools from extreme value theory. The frequency of spike occurrence is comparatively rare, spike events are contained in the tail of the corresponding spot price distribution, which makes reliable statistical inference rather difficult. Tools and methods from extreme value theory are designed to deal with these extreme events in that they compensate the lack of empirical information by a robust model approach based on probabilistic limit theorems.

We employ the proposed estimation procedure on daily EEX spot price data, and our findings are that spike risk must be modelled by distributions with fat tails of polynomial decay. This means that even when price jumps are introduced into a model by some compound Poisson process with Gaussian or exponentially distributed shocks (as is typically done in the literature, see e.g. [8], [11]), spike risk is still significantly underestimated.

Our paper is organized as follows. After listing the stylized facts of electricity data we present our model in Section 2. In Section 3 we summarize results from extreme value statistics, which we use to estimate the spike component of our model. This is done in Section 4, together with the fit of the base component. We conclude with a small simulation study, which shows the performance of our estimation method.

2. The spot price model

For daily electricity spot prices one observes a number of stylized features that a model should be able to capture. In [12] spot prices from European electricity exchanges have been analyzed and the following list of qualitative characteristics has been identified:

- **Seasonality.** Electricity spot prices reveal seasonal behavior both in yearly, weekly and daily cycles.
- **Stationarity.** Contrary to stock prices, electricity prices tend to exhibit stationary behavior. Similarly to other commodities, they are mean reverting to a trend which, however, may exhibit slow stochastic variations.
- **Multiscale autocorrelation.** The observed autocorrelation structure of most European price series is described quite precisely with a weighted sum of exponentials:

$$\widehat{\rho}(h) = \sum_{i=1}^{n} w_i e^{-h\lambda_i} .$$

Here $\widehat{\rho}(h)$ denotes the estimated autocorrelation function (acf) with lag h, and the number n of factors needed for a good description is 2 or 3. The weights w_i add up to 1.

- **Spikes.** Electricity spot prices show impressive spikes, that is violent upward jumps followed by rapid return to about the same level. The intensity of spike occurrence can vary over time. This fundamental property of electricity prices is due to the non-storability of this commodity.
- **Non-Gaussianity.** The examination of daily spot prices reveals a highly non-Gaussian distribution which tends to be slightly positively skewed and strongly leptokurtic. This high excess kurtosis is explained by the presence of the low-probability large-amplitude spikes.

The spot price model we want to consider in this paper is a multifactor model that has been introduced in [3]. Let $S(t)$ be the spot price at time t. Then $S(\cdot)$ is described by a

sum of non-Gaussian Orstein-Uhlenbeck processes (hereafter denoted as OU processes):

$$S(t) = \Lambda(t) \sum_{i=1}^{n} Y_i(t)\,, \quad t \geq 0\,, \tag{2.1}$$

where each process Y_i is the solution to the OU equation

$$dY_i(t) = -\lambda_i Y_i(t)\,dt + dL_i(t). \tag{2.2}$$

The function Λ denotes a deterministic seasonality function, and the L_i's are independent, increasing, possibly time inhomogeneous, pure jump Lévy processes. The increasing nature of the L_i guarantees positive prices despite of the arithmetic structure of the model. The compensating measure $\mu_i(dt, dz)$ of L_i is supposed to be of the form

$$\mu_i(dt, dz) = \rho_i(t)\,dt\,\nu_i(dz)\,,$$

where the deterministic function $\rho_i(\cdot)$ controls the possibly time varying jump intensity and $\nu_i(dz)$ is a Lévy measure with positive support. The parameter λ_i controls the rate of mean reversion of the factor Y_i. The different OU factors Y_i represent the price behavior on different time scales. Typically, three factors are sufficient for a good description: a first one for short term spike behavior with high mean reversion, a second one for medium term behavior, and a third one for long term variation with low mean reversion.

We recall that, given $Y_i(s)$, the explicit solution of the OU equation (2.2) for $Y_i(t)$ is given by

$$Y_i(t) = e^{-(t-s)\lambda_i} Y_i(s) + \int_s^t e^{-(t-r)\lambda_i} dL_i(r)\,, \quad s < t\,. \tag{2.3}$$

Further, if for all $i = 1, \ldots, n$ the jump intensities $\rho_i(t) = \rho_i$ are constant, then the L_i are time homogeneous Lévy processes and (2.2) admits a stationary solution, given the following logarithmic integrability condition on the Lévy measures

$$\int_{|z|>1} \ln(z)\,\nu_i(dz) \,<\, \infty\,, \quad i = 1, \ldots, n\,.$$

In that case the sum $\sum_{i=1}^n Y_i$ of OU processes exhibits the desired multiscale autocorrelation structure (provided the acf exists) given as

$$\rho(h) := \sum_{i=1}^{n} w_i e^{-h\lambda_i}\,; \qquad w_i = \frac{\operatorname{Var} Y_i(1)}{\sum_{j=1}^n \operatorname{Var} Y_j(1)}\,, \quad i = 1, \ldots, n. \tag{2.4}$$

The spot price model in (2.1) is sufficiently flexible to capture both the distributional as well as the path properties of electricity spot prices listed above. However, because the model is not Markovian, statistical estimation is not obvious. In [12] an estimation method for the model based on results from non-parametric statistics is presented. In the present paper, we want to develop an estimation procedure that invokes results and tools from extreme value theory. The violent spike behavior of electricity prices constitutes a significant risk for agents on energy markets. In order to be able to identify and to

manage that risk it is thus essential to thoroughly analyze the tail behavior of the price distribution. By employing tools from extreme value theory we will be able to provide a model specification and an estimation procedure that appropriately accounts for spike risk in the distribution tails.

In the next section we will give a short review of those results from extreme value theory we are going to use, before we present our estimation method in Section 4.

3. Some results from extreme value theory

The following gives a short review of results from extreme value statistics, which we are going to employ in the next section for the analysis of price spikes. In particular we are interested in *exceedances over a high threshold*, including diagnostical tools and estimation methods. For more details and further references of extreme value theory we refer to [6] or any other extreme value statistics monograph.

3.1. **Exceedances over high thresholds.**

Consider a sequence of i.i.d. random variables $(X_i)_{i\in\mathbb{N}}$ with common distribution function F. We are interested in the conditional distribution of X above a high threshold u, i.e.

$$F_u(x) = P(X - u \le x \mid X > u) = \frac{F(x+u) - F(u)}{1 - F(u)}\,, \quad x \in \mathbb{R}\,.$$

F_u is called the *excess distribution over threshold u*. As u approaches $x_F = \sup\{x : F(x) < 1\}$, one often finds a limit distribution function

$$\lim_{u \nearrow x_F} F_u(x) = G_{\xi,\beta}(x)\,, \quad x \in \mathbb{R}\,.$$

More precisely, this limit exists exactly for those F that belong to the so called maximum domain of attraction of the generalized extreme value distribution. In this case $G_{\xi,\beta}$ is the *generalized Pareto distribution* (GPD) defined as

$$G_{\xi,\beta}(x) = \begin{cases} 1 - (1 + \frac{\xi x}{\beta})^{-\frac{1}{\xi}}, & \xi \neq 0 \\ 1 - \exp(-\frac{x}{\beta}), & \xi = 0, \end{cases} \tag{3.1}$$

where $\beta > 0$, $x \ge 0$ for $\xi \ge 0$ and $0 \le x \le -\beta/\xi$ for $\xi < 0$. We call ξ the shape parameter and β the scale parameter. Notice that for $\xi > 0$, the GPD is equal to a Pareto distribution.

It can be shown, that $E(X^k) = \infty$ for $k \ge 1/\xi$. Thus, for a stationary stochastic process with marginal distribution function F as above, for $\xi \ge 0.5$, variance and autocorrelation function are not defined and one has to be careful when drawing conclusions from empirical autocorrelation functions.

3.2. **Estimation.** Now assume that $X_1, X_2, \ldots, X_n$ are i.i.d. with excess distribution function $F_u = G_{\xi,\beta}$. This is clearly an idealisation, since the excess distribution is generally only GPD in the limit. The parameters ξ and β are estimated by fitting $F_u = G_{\xi,\beta}$ to the exceedances over the treshold u, i.e. $(X_{(1)} - u, X_{(2)} - u, \ldots, X_{(k)} - u)$, where k equals the number of observations greater than u and $X_{(1)} > \cdots > X_{(k)}$ are the upper k order statistics. In practice, the threshold u has to be chosen appropriately, usually some high order statistic $X_{(k)}$ is taken. To choose k small brings us closer to the limit model, but we pay with a high variance for lack of data, to choose k at least moderate results in a more stable estimate, but we face a high bias for working with a probably wrong model. There exist data driven optimization methods to solve the involved mean-variance problem; see [2], Section 5.8. However, such methods can give disastrously wrong results. The usual remedy is to find a reasonable smallest threshold u through the mean excess plot. Since the mean excess function is linear if and only if X follows a generalized Pareto distribution, the mean excess plot should be approximately linear for $x > u$. Then the choice of u is based on a plot of the estimator versus the threshold u or the number of order statistics k used, where one can choose the estimator $\widehat{\xi}$ in dependence of u in an optimal way. The following are frequently used estimators for ξ (see e.g. [6], Chapter 6).

Maximum likelihood estimator (MLE): Writing $g_{\xi,\beta}$ for the density of the GPD, the log-likelihood is given by

$$\begin{aligned}\ln L(\xi, \beta \mid X_{(1)} - u, X_{(2)} - u, \ldots, X_{(k)} - u) &= \sum_{j=1}^{k} \ln g_{\xi,\beta}(X_{(j)} - u) \\ &= -k \ln \beta - \left(1 + \frac{1}{\xi}\right) \sum_{j=1}^{k} \ln \left(1 + \xi \frac{\xi}{\beta}(X_{(j)} - u)\right)\end{aligned}$$

Maximising subject to the constraints $\beta > 0$ and $(1 + \xi \frac{\xi}{\beta}(X_{(j)} - u)) > 0$ gives the MLEs $\widehat{\xi}_{ML}$ and $\widehat{\beta}$. Recall that under weak regularity conditions MLEs are consistent and asymptotically normal. However, these are asymptotic properties, which require a large number k of exceedances over u. Moreover, consistency is guaranteed for $\xi < 1$ and asymptotic normality only holds for $\xi < 0.5$. As the properties of these estimators for small samples are not clear, the following alternatives have been considered, concentrating first on the important shape parameter.

Hill estimator: Note first that it is defined only for $\xi > 0$. It is based on the fact that for a Pareto distributed random variable X with distribution tail $P(X > x) = x^{-1/\xi}$ for some threshold $u > 1$ we have $P(\ln X > y) = e^{-y/\xi}$ for $y = \ln u > 0$. Then it invokes the mean excess function, which is defined for any positive random variable Y as

$$e(y) = E(Y - y \mid Y > y)\,, \quad y > 0\,.$$

For the exponential distribution with parameter ξ we have $e(y) = \xi$ for all $y > 0$. The Hill estimator now conditions these facts on values above the threshold u, and considers

the empirical mean excess function over the threshold u giving

$$\widehat{\xi}_{Hill}(u) = \frac{1}{k}\sum_{j=1}^{k}\left(\ln X_{(j)} - \ln u\right).$$

Regression estimator based on mean excess plot: For $\xi < 1$ the mean excess function of a GPD random variable X is given by

$$e(u) = \frac{\beta + \xi u}{1-\xi}, \quad \beta + \xi u > 0;$$

cf. [6], Theorem 3.4.13(e). The corresponding estimator conditions these facts on values above the threshold u, and considers the empirical mean excess function over the threshold u, where it appears as approximately linear. The mean excess plot depicts the empirical version of $e(u)$ against u. Thus, from the slope of the linear regression line of the mean excess plot for values greater than u an estimator for ξ can be obtained. Let $\widehat{b}$ be the estimated slope of the linear regression line of the mean excess plot. Then the corresponding estimator is for ξ given by

$$\widehat{\xi}_{ME} = \frac{\widehat{b}}{1+\widehat{b}}.$$

For the linear regression, a robust linear regression [9] should be preferred to an OLS estimator. This estimates b by an iteratively reweighed least squares algorithm. It is less sensitive to changes towards the end of the range. These can disturb OLS estimates heavily due to the sparseness of the data available for estimating $e(u)$ for large u.

Regression estimator based on QQ-plot: For any random sample, a QQ-plot depicts the empirical quantiles versus the theoretical ones. This was exploited in [10] for a distribution function with far out Pareto tails, and applies to the GPD model above. It again exploits the fact that for X Pareto distributed with shape parameter ξ, $\ln X$ is exponentially distributed with parameter ξ. The resulting estimator is given by

$$\widehat{\xi}_{QQ}(u) = \frac{\sum_{j=1}^{k} -\ln\left(1-\frac{j}{k+1}\right)\left(k\ln(X_{(j)}-u) - \sum_{j=1}^{k}\ln(X_{(j)}-u)\right)}{k\sum_{j=1}^{k}\left(-\ln\left(1-\frac{j}{k+1}\right)\right)^2 - \left(\sum_{j=1}^{k} -\ln\left(1-\frac{j}{k+1}\right)\right)^2},$$

which is the slope of the regression line of

$$\left(-\ln\left(1-\frac{j}{k+1}\right), \ln\left(X_{(j)}-u\right)\right), \quad 1 \le j \le k.$$

Again we recommend a robust estimator for the same reasons as for the mean excess plot.

After having estimated the shape parameter ξ, we also have to estimate the corresponding scale parameter β of the GPD. This can be done by using a conditional likelihood, conditioning on the estimate $\widehat{\xi}$.

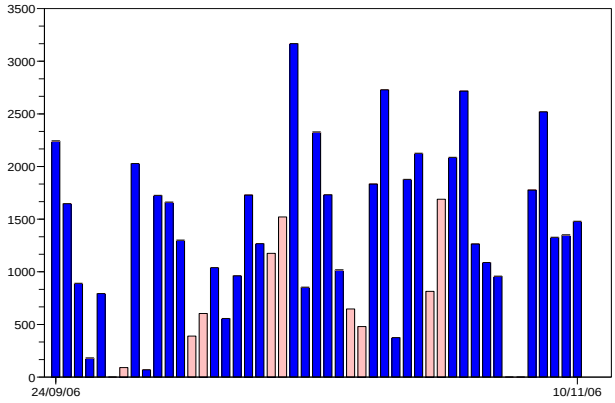

FIGURE 4. Daily trade volume, in MWh, on the EEX market, from 24/09/2006 to 10/11/2006. Bright-colored bars correspond to weekends. Data are downloaded from EEX website at `www.eex.de`.

4. Estimation and simulation

In this section we will develop a procedure to estimate our spot price model (2.1). In particular, we will use the tools from extreme value theory presented in Section 3 in order to identify and to model the spike component. We employ this procedure to estimate the model for the European Power Exchange Phelix Base electricity price index (EEX) (see Figure 5).

The data is daily EEX spot prices provided by Datastream, running from 16/06/2000 to 21/11/2006 exluding weekends. Contrary to stocks, electricity is traded also on weekends, however in much smaller volumes than on week days (see Figure 4). This causes a significant difference in Friday-to-Monday price behavior compared to intra-week price behavior. However, while weekends introduce a lot of seasonality, they do not account for interesting statistical features (e.g., no spikes during weekends). In order to make deseasonalising easier we decided to consider data without weekends.

The EEX data series exhibits all of the in Section 2 listed stylized features of electricity spot prices. In particular, Figure 5 illustrates clearly the occurrence of very large amplitude spikes from time to time during which price levels can increase by a factor of 10 in the course of a day. Further, Table 2 confirms that the data is highly non-Gaussian with an overall excess kurtosis of 36.93 (recall that the normal distribution has excess kurtosis 3).

Exchange	Mean	StD	Skewness	Kurtosis
EEX	**35.86**	**20.08**	**4.10**	**36.93**
summer (Apr - Sep)	33.85	17.77	6.04	77.63
winter (Oct - Mar)	37.97	22.06	2.93	17.69

TABLE 2. Summary statistics for daily system prices

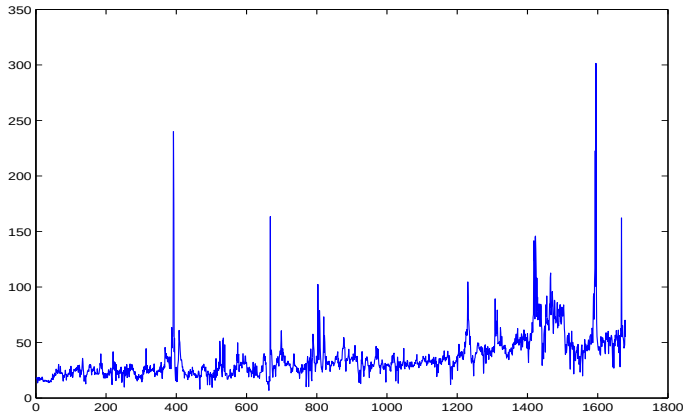

FIGURE 5. Daily EEX Phelix Base electricity price index from 16/06/2000 to 10/11/2006.

4.1. **Model estimation.** We now present a procedure how to specify and estimate model (2.1) for the EEX data. We will in the following assume time homogenous Lévy processes in (2.2) to model EEX prices, an assumption that will be discussed in the course of this section. Let $S(t)$ denote the spot price at time t and t_j for $j = 1, \ldots, N$ the equally spaced daily observation times, where in the case of the EEX data $N = 1679$.

For notational simplicity we define $S(j) := S(t_j)$ (and respectively for any other time series). We divide the estimation procedure into three steps.

Step 1 *(Deseasonalizing the data)*: We assume a continuous seasonality function of cosines including a trend, a weekly, and a yearly cycle of the form $\Lambda(t) = \exp(g(t))$ with

$$g(t) = \beta_0 + \beta_1 \cos\left(\frac{\tau_1 + 2\pi t}{260}\right) + \beta_2 \cos\left(\frac{\tau_2 + 2\pi t}{5}\right) + \beta_3 t\,, \quad t \geq 0\,.$$

We estimate the seasonality function by fitting $g(t)$ to log-prices using robust least squares estimation. Here, robust simply means that outliers are cut off as long as they have a significant impact on the estimation of $g(\cdot)$. The algorithm we use is based on the following iteration: In the first step, the function $g(\cdot)$ is fitted to $\ln S(\cdot)$ with an ordinary least squares estimation. In each iteration step we only consider log-prices $\ln(S(i))$ that lie within a certain band around the estimated function $\widehat{g}_{i-1}(\cdot)$ of the previous step, i.e. in the ith iteration, the seasonality function $g(j)$ for $j = 1, \ldots, N$ is fitted to the data

$$\begin{array}{ll} \ln S(j) & \text{if } \widehat{g}_{i-1}(j) - 1.5\,s < \ln S(j) < \widehat{g}_{i-1}(j) + 1.5\,s\,, \\ \widehat{g}_{i-1}(j) + 1.5\,s & \text{if } \ln S(j) > \widehat{g}_{i-1}(j) + 1.5\,s\,, \\ \widehat{g}_{i-1}(j) - 1.5\,s & \text{if } \ln S(j) < \widehat{g}_{i-1}(j) - 1.5\,s\,, \end{array}$$

where $\widehat{g}_{i-1}(j)$ denotes the estimation of the previous iteration and s the standard deviation of the residuals of the previous iteration. The iteration ends, when two subsequent estimations are sufficiently close together, i.e. when $\sum_{j=1}^{N} \left(\widehat{g}_i(j) - \widehat{g}_{j-1}(t)\right)^2 < 0.01$.

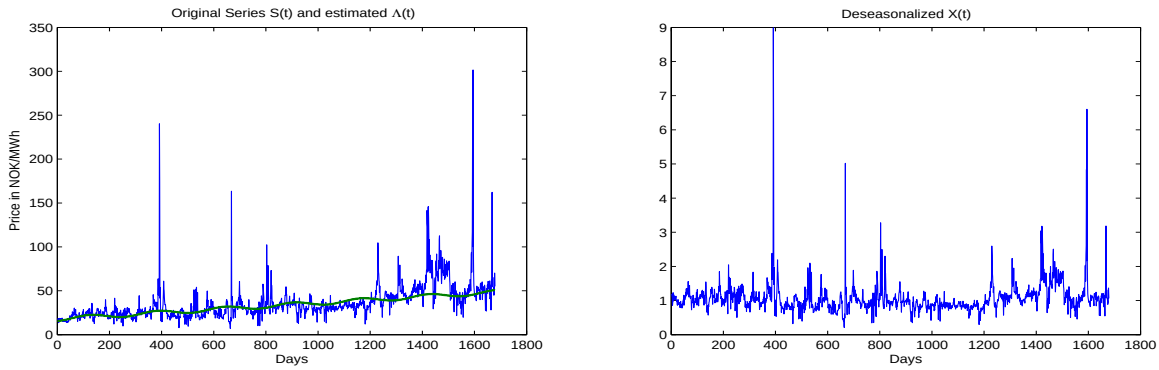

FIGURE 6. Left: Original series $S(\cdot)$ and estimated $\widehat{\Lambda}(\cdot)$. Right: Deseasonalized series $X(\cdot)$.

The deseasonalized spot price (see Figure 6) is then denoted as

$$X(t) := \frac{S(t)}{\widehat{\Lambda}(t)}, \quad t \geq 0,$$

where $\widehat{\Lambda}(\cdot)$ is the estimated seasonality function.

Step 2 *(Spike identification)*: Next, because of the non-Markovianity of the model, efficient estimation requires the separation of the data $X(\cdot) = X_1(\cdot) + X_2(\cdot)$ into a spike component $X_1(\cdot)$, which is supposed to be modelled by the first factor $Y_1(\cdot)$ in (2.1), and a remaining base component $X_2(\cdot)$.

We start by assessing the rate λ_1 with which the spot price mean reverts to the base component, when a spike occurs.

Let $Y(j)$ for $j = 1, \ldots, N$ be equally spaced discrete observations with time space Δ of an OU process

$$dY(t) = -\lambda Y(t)dt + dL(t),$$

which is driven by an increasing Lévy process L. Then one can estimate λ with the Davis-McCormick estimator given as

$$\widehat{\lambda} = \frac{1}{\Delta} \ln \left(\max_{1 \leq j \leq N} \frac{Y(j-1)}{Y(j)} \right). \tag{4.1}$$

For every stationary OU process this estimator is weakly consistent as $N \to \infty$ with Δ fixed, and it has a limiting distribution under certain assumptions on the distribution of $\int_0^1 e^{-\lambda(1-s)} dL(s)$; see [4] and references therein. Our estimation of λ_1 is, however, based on some isolated peaks, so that asymptotic properties are not relevant. One property of the estimator is, however, that $\widehat{\lambda} \leq \lambda$, hence $\widehat{\lambda}$ is biased downwards.

Consequently, if we observed the OU spike path $X_1(j)$ for $j = 1, \ldots, N$, then we could estimate the corresponding rate of mean reversion λ_1 by

$$\ln \left(\max_{1 \leq j \leq N} \frac{X_1(j-1)}{X_1(j)} \right).$$

However, in our situation we do not observe $X_1(j)$ but only the sum $X(j) = X_1(j)+X_2(j)$, whose ratio is given as

$$\frac{X(j)}{X(j-1)} = \frac{X_1(j)+X_2(j)}{X_1(j-1)+X_2(j-1)} = \frac{X_1(j)}{X_1(j-1)}\left(1-\frac{X_2(j-1)}{X(j-1)}\right)+\frac{X_2(j)}{X(j-1)}.$$

Now we observe that, asymptotically for $X(j-1)\to\infty$ the correction terms $\frac{X_2(j-1)}{X(j-1)}$ and $\frac{X_2(j)}{X(j-1)}$ tend to zero. This leads us to use

$$\widehat{\lambda}_1 = \ln\left(\max_{j\in\mathcal{J}}\frac{X(j-1)}{X(j)}\right)$$

as an estimator for spike mean reversion, where $\mathcal{J}$ is the set of time points such that $X(j) > v$ for a treshold $v > 0$. The treshold v has to be chosen such that the big spikes are included. For our data set, the maximal ratio is obtained for the biggest spike around day 400 and we find $\widehat{\lambda}_1 = 1.39$.

We now proceed to disentangle the deseasonalized data $X = X_1 + X_2$ into a spike component X_1 and base component X_2. This will be done by employing tools from extreme value statistics to design a treshold method that filters out spike jumps. That is, given that price variation is above a certain treshold, we assume this variation is caused by a spike jump. Motivated by the asymptotic results of Section 3.1, we determine the threshold such that the spike jump distribution, i.e. the Lévy measure $\nu_1(dz)$ of L_1, is well described through the *generalized Pareto distribution* (GPD) from extreme value theory. More precisely, we model L_1 as a compound Poisson process with rate ρ_1 (to be specified later) and a GPD jump distribution with shape parameter $\xi > 0$.

In order to identify spike jumps in X we consider for known λ_1 the autoregressive transformation

$$Z(j) := X(j) - e^{-\lambda_1}X(j-1)\,,\quad j = 1,\dots,N\,. \tag{4.2}$$

Then, as easily seen from (2.3), Z is modelled as

$$Z(j) = X_2(j) - e^{-\lambda_1}X_2(j-1) + \epsilon(j)\,,\quad j = 1,\dots,N\,, \tag{4.3}$$

where all $\epsilon(j)$ have the same distribution as $\int_0^1 e^{-\lambda_1(1-s)}dL_1(s)$ and represent the i.i.d. spike jumps. Note that $\varepsilon(j)$ will be zero most of the time, namely, whenever X is in the base regime. Only if $Z(j)$ is above a certain threshold, say u, we assume a spike jump has occurred, corresponding to $\varepsilon(j) > 0$.

Next we want to estimate the spike jump $\epsilon(j)$ from (4.3), but face the problem that $X_2(j)$ is unknown. By assuming stationarity of $X_2(\cdot)$ (and we shall see that this is justified) we first replace each $X_2(j)$ forall $j = 1,\dots,N$ by its arithmetic mean. Further, we replace the mean reversion rate λ_1 with its estimation $\widehat{\lambda}_1$, which yields the estimate

$$\widehat{\epsilon}(j) = \left(Z(j) - (1-e^{-\widehat{\lambda}_1})\frac{1}{N}\sum_{i=1}^{N}X_2(i)\right)I_{Z(j)>u}\,. \tag{4.4}$$

But as already mentioned, we cannot observe $X_2(j)$ or their mean directly but only the sum $X_1(j)+X_2(j)$. However, with an estimated spike mean reversion rate $\widehat{\lambda}_1 = 1.39$, the impact of a spike on spot prices vanishes by 94% within the first two days. Consequently we can take the arithmetic mean over all data points excluding the first two consecutive days following a spike jump occurrence. Let M be the length of this adjusted time series. Then we replace the estimation in (4.4) by

$$\widehat{\epsilon}(j) = \left(Z(j) - (1 - e^{-\widehat{\lambda}_1}) \frac{1}{M} \sum_{i=2}^{N} X(i) I_{(Z(i-1)\leq u \text{ and } Z(i)\leq u)} \right) I_{Z(j)>u} \,. \tag{4.5}$$

The spike path X_1 is then built following the OU dynamics (2.3) as

$$X_1(j) = e^{-\widehat{\lambda}_1} X_1(j-1) + \widehat{\epsilon}(j)\,, \quad j = 1, \ldots, N\,, \tag{4.6}$$

with initialization $X_1(0) = \widehat{\epsilon}(0)$. Finally, the base component X_2 is constructed as

$$X_2(j) = X(j) - X_1(j)\,, \quad j = 1, \ldots, N\,. \tag{4.7}$$

The essential and remaining task in the above described procedure to filter out the spike path is the choice of the treshold u. Using the diagnostic and estimation tools from extreme value theory presented in Section 3, we propose to determine the treshold u in such a way that the filtered spike jumps are well fitted by a (shifted) GPD. More precisely, we determine u such that the exceedances $(Z(j)-u)I_{Z(j)>u}$ are well described by a GPD. From (4.4) we then obtain that the jump size distribution in the compound Poisson process L_1 is a shifted GPD with left endpoint L given by the estimation in (4.5) as

$$\widehat{L} = u - (1 - e^{-\widehat{\lambda}_1}) \frac{1}{M} \sum_{i=2}^{N} X(j) I_{(Z(i-1)\leq u \text{ and } Z(i)\leq u)} \,. \tag{4.8}$$

The mean excess plot performed on $Z(j)$ for $j = 1, \ldots, N$ in Figure 7 exhibits approximately a linear slope for thresholds bigger than 0.8 and, consequently, we should choose $u \geq 0.8$. For the estimation of the GPD parameters ξ and β we invoke methods presented in Section 3.2.

We first concentrate on the estimator for the shape parameter ξ, which we plot as functions $\widehat{\xi}(u)$ of the threshold in Figure 8. From the very definition, it is clear that the plots based on the Hill and ML estimators vary in a non-smooth way with the number of order statistics used. The two regression estimators, on the other hand, change more smoothly, but they are more curved exactly for high thresholds, in particular the one based on the mean excess plot. Consequently, we choose to read off a particular value rather from the MLE plot than from any other plot. Also, from a risk management point of view, choosing the MLE secures against the 'worst case' because the MLE proposes the highest values for ξ. Nonetheless, combining all plots we can conclude that for a reasonably high threshold ξ lies between 1/3 and 1/2, which implies that we have a finite second moment,

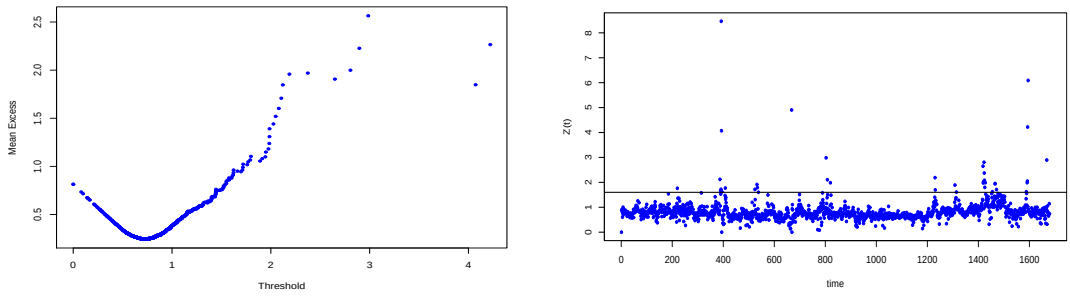

FIGURE 7. Left: ME plot of $Z(\cdot)$, right: $Z(\cdot)$ with chosen threshold $u = 1.62$.

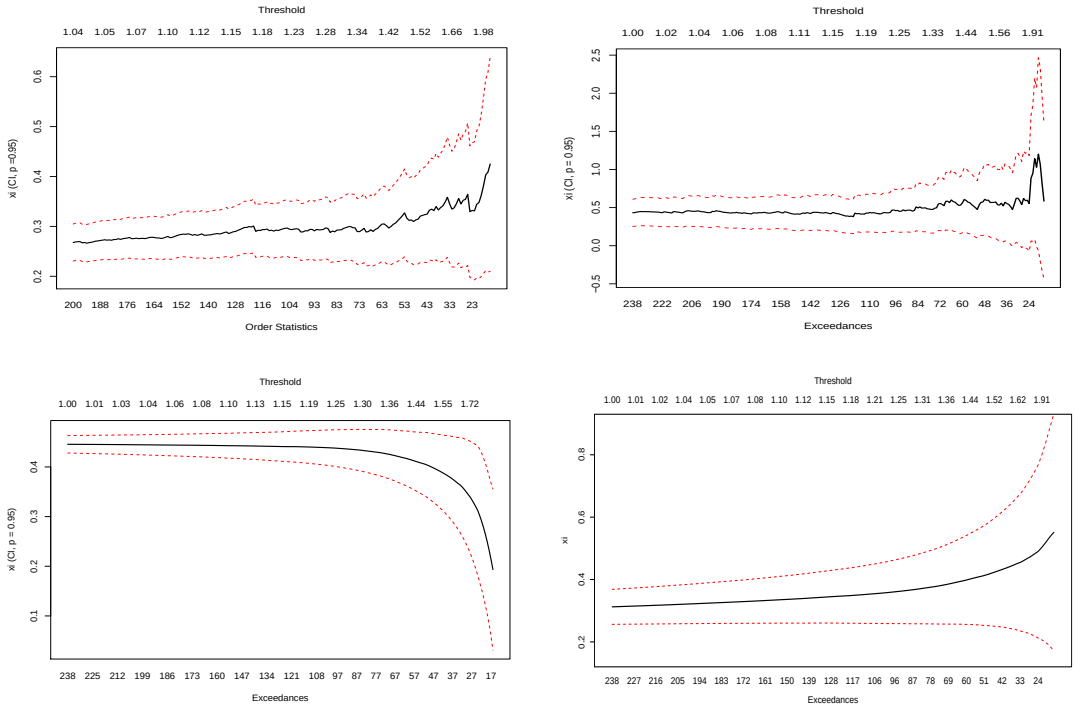

FIGURE 8. Different estimates of ξ for different thresholds with asymptotic 95% pointwise confidence bands: left: $\widehat{\xi}_{Hill}$, right: $\widehat{\xi}_{MLE}$, lower left: $\widehat{\xi}_{ME}$, lower right: $\widehat{\xi}_{QQ}$.

but an infinite third moment. We fix our parameters by choosing $u = 1.62$ and obtain the MLEs $\widehat{\xi} = 0.47$ and $\widehat{\beta} = 0.51$. Finally, we estimate the left endpoint of the GPD by the empirical counterpart of (4.8), which is not efficient, but for our purpose sufficiently close.

Remark 4.1. (1) For illustration we also depict the estimated GPD quantile function based on the four estimation methods from above for the same threshold $u = 1.62$. Although the estimators for ξ and β are fairly different, the estimated quantile functions in the relevant risk management area as depicted in Figure 9 are remarkably close.

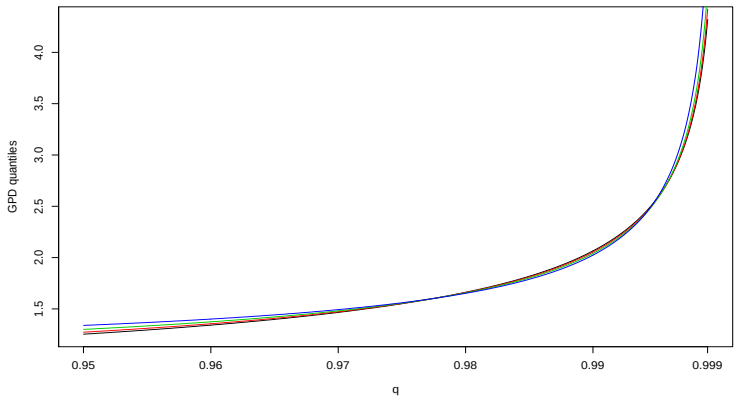

FIGURE 9. Four different estimates of the quantile function in the relevant risk management area based on the above different estimates for ξ and β for threshold $u = 1.62$.

(2) Our explorative analysis clearly indicates that appropriate modelling of spike risk requires a Pareto-like distribution with polynomial tail. We want thus to emphasize that jump diffusion type models which account for jump behavior through the introduction of a compound Poisson process with exponential or Gaussian shocks (as is typically done in the literature; cf. [8, 11]) significantly underestimate spike risk. This can be seen from the empirical mean excess function in Figure 7. For an exponential distribution the mean excess function is constant, whereas for the normal distribution it decreases to 0.

The last parameter we have to identify in order to complete the specification of the first factor $Y_1(\cdot)$ is the jump intensity ρ_1. We cannot detect any significant seasonal behavior in spike occurrence. Consequently, we work with a constant instead of a time varying intensity ρ_1, which is estimated simply as

$$\widehat{\rho}_1(t) = \widehat{\rho}_1 = \frac{1}{N}\text{card}\{j \,:\, Z(j) \geq u\,,\, j = 1, \ldots, N\}\,.$$

For our treshold $u = 1.62$ we count 38 spike jumps $\epsilon(j) > 0$ for $i = 1, \ldots, 38$ (see Figure 7), which implies a jump intensity $\widehat{\rho}_1 = 0.023$.

We want to remark that in the right hand Figure 7 exceedances over thresholds seem to appear in clusters, which then cannot be modelled by a Poisson process. This would suggest the introduction of a stochastic spike jump intensity $\rho_1(t, \omega)$. This is, however, beyond the scope of this paper and left for future research.

Finally, Figure 10 shows the corresponding separation of the deseasonalized spot prices into the spike component X_1 and the base component X_2.

Step 3 *(Base component)*: Performing a Dickey-Fuller test as well as its augmented version (for details see [16]) on $\widehat{X}_2(j)$ for $j = 1, \ldots, n$ strongly suggests stationarity of the base component (see Table 3). We thus assume stationarity for the base component $X_2(\cdot)$, which we model as a sum of stationary OU processes.

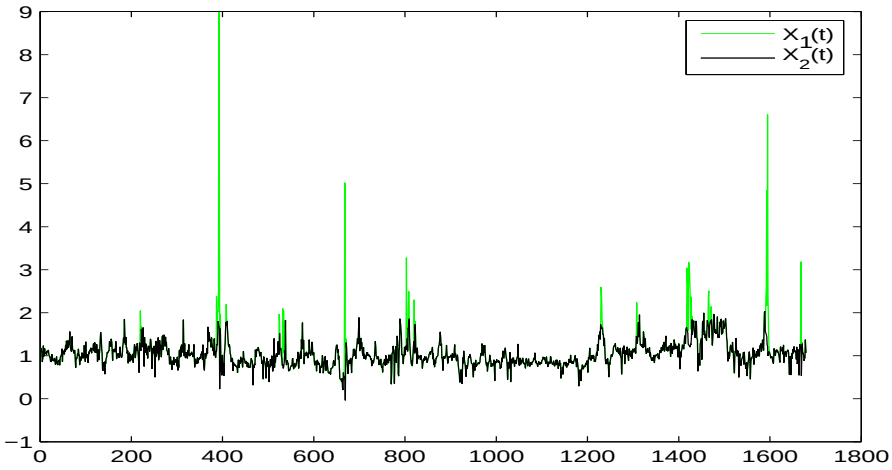

FIGURE 10. Decomposition of $X(\cdot)$ into the spike component $X_1(\cdot)$ and the base component $X_2(\cdot)$.

DF	ADF	95%-quantile
-14.7	-8.9	-2.86

TABLE 3. Dickey-Fuller and augmented Dickey-Fuller test results on $\widehat{X}_2(j)$ for $j = 1, \ldots, N$.

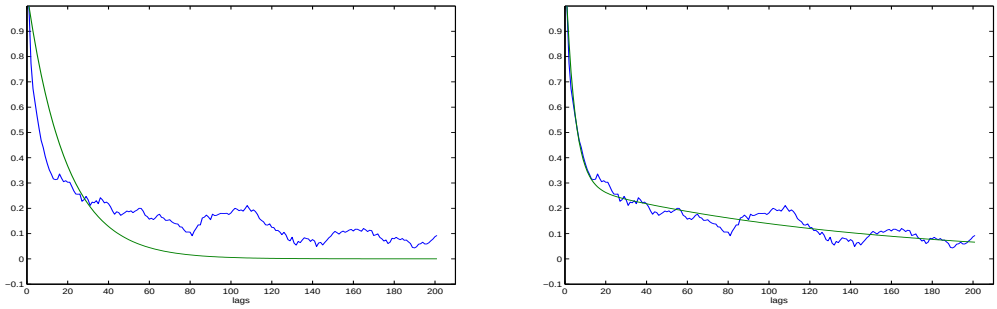

FIGURE 11. Left: Fit of the estimated autocorrelation function of X_2 with one factor. Right: Fit with two factors.

The number $n-1$ of remaining factors $Y_2, \ldots, Y_n$ necessary to model $X_2(\cdot)$ and their rates of mean reversion $\lambda_2, \ldots, \lambda_n$ are determined by analyzing the autocorrelation structure of $X_2(\cdot)$. Figure 11 demonstrates that a multiscale autocorrelation of the form (2.4) corresponding to two additional factors gives a good fit of the empirical autocorrelation; i.e. we model the base component as

$$X_2(t) = Y_2(t) + Y_3(t)\,, \quad t \geq 0\,.$$

The fit is based on least squares estimation, and Table 4 reports the corresponding estimated mean reversion rates $\widehat{\lambda}_2$ and $\widehat{\lambda}_3$ together with $\widehat{w}_2$ and $\widehat{w}_3$. This means that, additionally to the fast mean reverting spike factor Y_1, we need two more factors Y_2 and Y_3 with medium and slow mean reversion, respectively.

$\widehat{\lambda}_2$	$\widehat{\lambda}_3$	$\widehat{w}_2$	$\widehat{w}_3 = 1 - \widehat{w}_2$
0.243	0.0094	0.68	0.32

TABLE 4. Estimated parameters from fitting the model autocorrelation (2.4) to the empirical autocorrelation of the base component by robust least squares.

We conclude the estimation procedure with the remaining specification of jump intensities ρ_2, ρ_3 and Lévy measures $\nu_2(dz)$, $\nu_3(dz)$. For this purpose, we first fit the stationary marginal distribution of the base component to $X_2(j) = Y_2(j) + Y_3(j)$ for $j = 1, \ldots, n$ using quasi-MLE (QMLE). More precisely, we assume that the stationary distribution of $Y_2(\cdot) + Y_3(\cdot)$ is given by a density $f_\theta(\cdot)$ with parameter vector θ, which is estimated by

$$\widehat{\theta} = \arg\max_\theta \prod_{j=1}^{n} f_\theta(X_2(j))\,. \tag{4.9}$$

The term quasi-MLE is used because the data $X_2(1), \ldots, X_2(n)$ are not realizations of independent random variables. However, since the acf of $X_2(\cdot)$ is exponentially decreasing, the estimate in (4.9) has the same asymptotic properties as a classical MLE.

We work with a gamma distribution $\Gamma(a, b)$ with density $f(y) = b^a e^{-by} x^{a-1}/\Gamma(a)$ for $y > 0$ as statistical model of $Y_2(j) + Y_3(j)$ for $j = 1, \ldots, n$. Though the data shown in Figure 12 are slightly non-symmetric and leptokurtic, the gamma distribution provides an acceptable fit to the data $X_2(j)$ for $j = 1, \ldots, n$ and has the advantage that in this model the single factors are easy to fit and to simulate. QMLE yields a distribution $\Gamma(\widehat{a}, \widehat{b})$ for the sum $X_2(j) = Y_2(j) + Y_3(j)$ for $j = 1, \ldots, n$ with $\widehat{a} = 14.8$ and $\widehat{b} = 14.4$. In order to specify the single factors we assume distributions $\Gamma(a_2, b)$ and $\Gamma(a_3, b)$ for $Y_2(j)$ and $Y_3(j)$, respectively, such that $a_2 + a_3 = a$. Then the stationary distribution of the sum $X_2(j)$ is $\Gamma(a, b)$ as desired.

Finally, for $i = 1, 2$ we estimate the weights w_i and a_i from (2.4) together with the autocorrelation fit (see Table 4), which gives

$$\widehat{w}_2 \;=\; 0.68 \;=\; \frac{\widehat{a}_2}{\widehat{a}}\,.$$

This gives the unique specification $\Gamma(\widehat{w}_2\widehat{a}, \widehat{b})$ and $\Gamma(\widehat{w}_3\widehat{a}, \widehat{b})$ as stationary distributions for Y_2 and Y_3, respectively. Recall from [1] that this implies that the driving Lévy processes L_2 and L_3 are compound Poisson processes with jump intensities and Lévy measures

$$\rho_i = \lambda_i w_i a \quad \text{and} \quad \nu_i(dz) = be^{-bz} 1_{z>0}\, dz\,, \quad i = 1, 2\,.$$

This completes the specification and estimation of the model to EEX spot prices.

We summarize the estimation results of this section in Table 5.

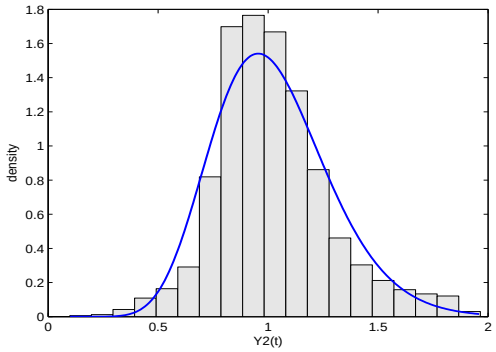

FIGURE 12. QML-fit of data $X_2(j) = Y_2(j) + Y_3(j)$ for $j = 1, \dots, n$ by a gamma distribution.

	mean reversion rate $\widehat{\lambda}_i$	jump intensity $\widehat{\rho}_i$	jump size density $\nu_i(dz)/dz$	parameters
Y_1	1.39	0.023	$\frac{1}{\beta}\Big(1 + (\frac{\xi}{\beta}(z - L))\Big)^{-\frac{1+\xi}{\xi}} 1_{z>0}$	$\widehat{\xi} = 0.47$ $\widehat{\beta} = 0.51$ $\widehat{L} = 0.83$
Y_2	0.243	2.446	$b\, e^{-b\, z} 1_{z>0}$	$\widehat{b} = 14.4$
Y_3	0.0094	0.045	$b\, e^{-b\, z} 1_{z>0}$	$\widehat{b} = 14.4$

TABLE 5. Summary of factor characteristics for model (2.1) from the estimation procedure.

4.2. **Simulation.** We conclude this section with a simulation study, where we simulate price paths scenarios of the deseasonalized spot price process $X(\cdot)$ using the model specifications from Table 5. More precisely, we simulate and add three OU factors of the type (2.3), which are driven by compound Poisson processes, a task that is easily performed. Estimating the three factors again is, however, a difficult problem, since mixture models are always difficult to decompose statistically into their different factors.

To start with a simple eye-test in Figure 13, we see that the simulated paths indeed mimic well the spot price behavior. Furthermore, the first four moments are acceptably reproduced as reported in Table 6.

	mean	**std**	**skew**	**kurt**
empirical moments	1.067	0.445	6.941	94.02
simulated moments	1.057	0.413	4.932	98.95

TABLE 6. Comparison of empirical and simulated moments (2000 simulations).

For a more serious analysis of our estimation procedure in Section 4.1 we simulated 100 sample paths of the deseasonalized spot price $X(\cdot)$ with parameter values given in Table 5 and apply our estimation procedure to every simulated path.

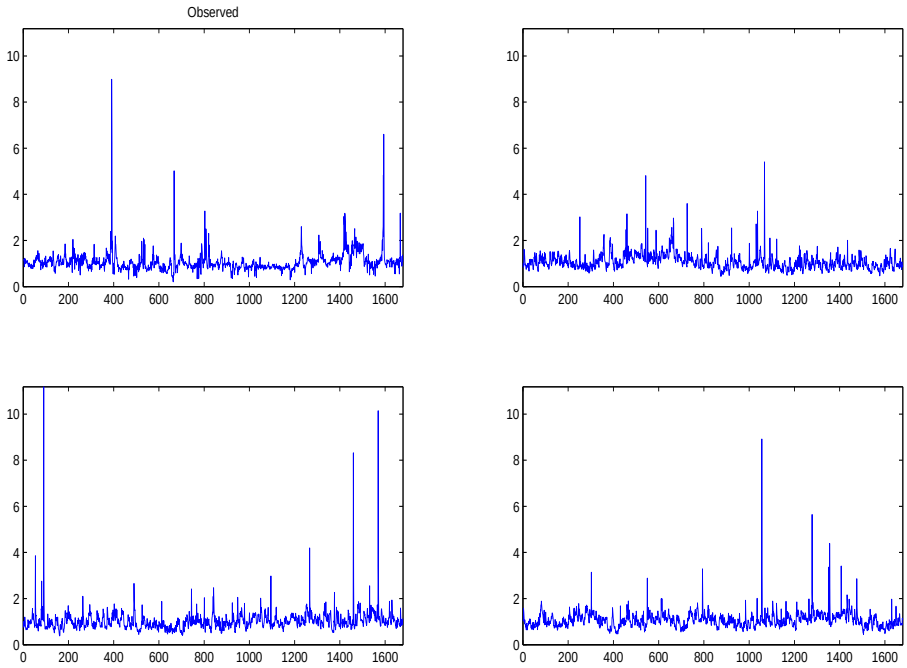

FIGURE 13. Three simulated paths in comparison with the data $X(\cdot)$ (top left)

We estimate first the spike component $X_1(\cdot)$ of (4.6) as explained in Step 2. Based on the 100 simulated sample paths we summarize the parameter estimation for $X_1(\cdot)$ in Table 5. Since the estimation is based on threshold data, as in every extreme value statistics procedure we expect to see rather high variation in the estimators. Furthermore, as stated in Step 2, $\widehat{\lambda}_1$ always underestimates λ_1. In Table 7 we present the mean, the mean squared error, and the mean relative bias of the estimated parameters.

In spite of all the drawbacks, as can be seen in Figure 14 for one specific sample path, our estimation procedure recovers the spike and base component rather convincingly.

	$\widehat{\lambda}_1$	$\widehat{\rho}_1$	$\widehat{\xi}$	$\widehat{\beta}$	$\widehat{L}$
Values	1.39	0.023	0.47	0.51	0.83
$\widehat{mean}$	1.2030 (0.2510)	0.0211 (0.0042)	0.5684 (0.1816)	0.4632 (0.2753)	0.8232 (0.0662)
$\widehat{MSE}$	0.0973 (0.1938)	0.0002 (0.0005)	0.0361 (0.0724)	0.0751 (0.1319)	0.0013 (0.0019)
$\widehat{MRB}$	−0.1345	−0.0828	0.1145	−0.0145	−0.0037

TABLE 7. Estimated mean, mean squared error (MSE) and mean relative bias (MRB) of estimated parameters for $X_1(\cdot)$ as in (4.6) from 100 simulated paths with estimated standard deviations for mean and MSE in brackets.

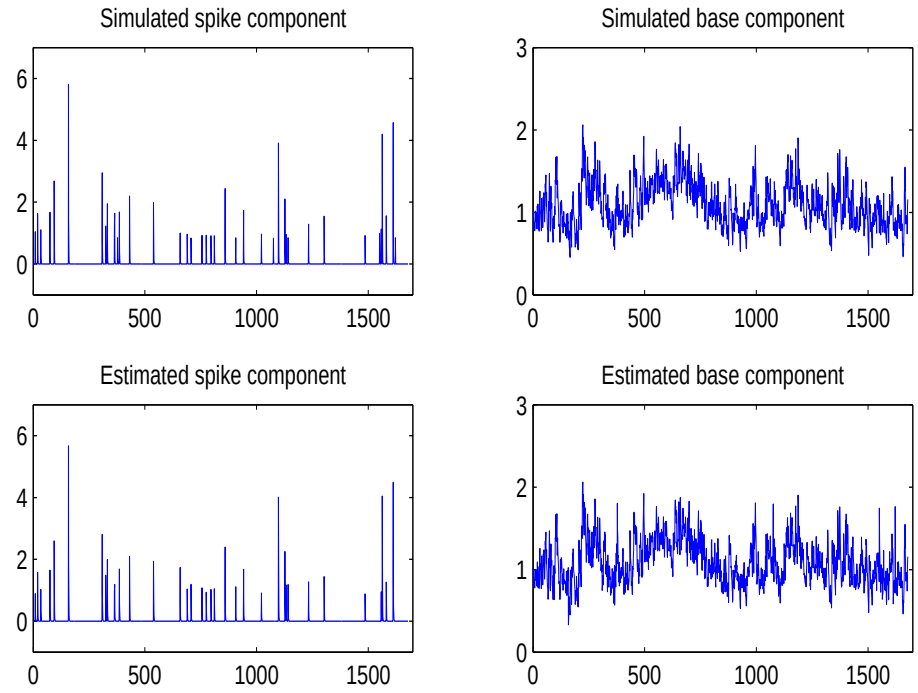

FIGURE 14. The true (top) in comparison with estimated (bottom) spike and base component for one simulated spot price path.

Next for every simulated sample path we subtracted the estimated spike component resulting in the two-factor model $X_2(\cdot)$ as in (4.7), and we estimated all parameters as described in Step 3. The fact that it is still a mixture model affects in particular the estimation of λ_2 and λ_3, but also a_2 and a_3, whereas a and b are slightly overestimated in mean, but perform reasonably well. The results are documented in Table 8.

	$\widehat{\lambda}_2$	$\widehat{\lambda}_3$	$\widehat{a}_2$	$\widehat{a}_3$	$\widehat{a}$	$\widehat{b}$
Values	0.243	0.0094	10.07	4.79	14.8	14.4
$\widehat{mean}$	0.2664 (0.1086)	0.0172 (0.0254)	10.9752 (3.0228)	4.6554 (2.3204)	15.6335 (1.7587)	15.1858 (1.7395)
$\widehat{MSE}$	0.0122 (0.0640)	0.0007 (0.0035)	9.8729 (15.8091)	5.3479 (13.5578)	3.6669 (5.6636)	3.6130 (5.5364)
$\widehat{MRB}$	0.0965	0.8272	0.0903	−0.0275	0.0524	0.0546

TABLE 8. Estimated mean, mean squared error (MSE) and mean relative bias (MRB) of estimated parameter sets for $X_2(\cdot)$ and $X_3(\cdot)$ from 100 simulated sample paths with estimated standard deviations for mean and MSE in brackets.

References

[1] Barndorff-Nielsen, O. and Shephard, N. (2001) Non-Gaussian Ornstein-Uhlenbeck based models and some of their uses in financial economics (with discussion). *Journal of the Royal Statistical Soiety B* **63**(2), 167-241.

[2] Beirlant, J., Goegebeur, Y., Segers, J. and Teugels, J. (2004) *Statistics of Extremes.* Wiley, Chichester.

[3] Benth F.E., Meyer-Brandis T. and Kallsen J. (2007) A non-Gaussian Ornstein-Uhlenbeck process for electricity spot price modeling and derivatives pricing. *Appl. Math. Fin.* **14**(2), 153-169.

[4] Brockwell, P. J., Davis, R. A. and Yang, Y. (2007) Estimation for non-negative Lévy-driven Ornstein-Uhlenbeck processes. *J. Appl. Probab.* **44**(4). To appear. Available at http://www-m4.ma.tum.de/Papers/

[5] Davis, R.A. and Resnick, S.I. (1986) Limit theory for the sample covariance and correlation functions of moving averages. *Ann. Statist.* **14**, 533-338.

[6] Embrechts, P., Klüppelberg, C. and Mikosch, T. (1997) *Modelling Extremal Events for Insurance and Finance.* Springer, Berlin.

[7] Geman, H. (2005) *Commodities and Commodity Derivatives.* Wiley, Chichester.

[8] Geman, H. and Roncoroni, A. (2006) Understanding the fine structure of electricity prices. *Journal of Business* **79**, 1225-1261.

[9] Huber, P.J. (2004) *Robust Statistics.* Wiley, New York.

[10] Kratz, M.F. and Resnick, S.I. (1996) The QQ-estimator and heavy tails. *Stochastic Models* **12**, 699-724.

[11] Lucia, J. and Schwartz, E. S. (2002) Electricity prices and power derivatives: evidence from the Nordic Power Exchange. *Rev. Derivatives Res.* **5**(1), 5-50.

[12] Meyer-Brandis, T. and Tankov, P. (2007) Statistical features of electricity prices: evidence from European energy exchanges. IJTAF, to appear.

[13] Nordel. (2007) Annual statistics 2006. Available at www.nordel.org.

[14] VDEW. (2006) Fakten - Informationen fur Journalisten. Available at www.vdew.org.

[15] von Hirschhausen, C., Weigt, H. and Zachmann, G. (2007) Price formation and market power in Germany's electricity markets. Study commissioned by *Association of German Industrial Energy Consumers.*

[16] Veerbeck, M. (2004) *A Guide to Modern Econometrics.* Wiley, Chichester.

(Claudia Klüppelberg), Center of Mathematical Sciences and Institute for Advanced Study, Technische Universität München, D-85747 Garching, Germany

E-mail address: cklu@ma.tum.de, URL: http://www-m4.ma.tum.de

(Thilo Meyer-Brandis), Center of Mathematics for Applications, University of Oslo, P.O. Box 1053, Blindern, N–0316 Oslo, Norway

E-mail address: meyerbr@math.uio.no

(Andrea Schmidt), Deutsche Bank AG, Global Markets, Groe Gallusstr. 10-14, 60272 Frankfurt, Germany